

The three body first post-Newtonian effects on the secular dynamics of a compact binary near a spinning supermassive black hole

Yun Fang^{1,2,*} and Qing-Guo Huang^{1,2,3,4,5,†}

¹*CAS Key Laboratory of Theoretical Physics, Institute of Theoretical Physics,
Chinese Academy of Sciences, Beijing 100190, China*

²*School of Physical Sciences, University of Chinese Academy of Sciences, No. 19A Yuquan Road, Beijing 100049, China*

³*School of Fundamental Physics and Mathematical Sciences Hangzhou
Institute for Advanced Study, UCAS, Hangzhou 310024, China*

⁴*Center for Gravitation and Cosmology, College of Physical Science
and Technology, Yangzhou University, Yangzhou 225009, China*

⁵*Synergetic Innovation Center for Quantum Effects and Applications,
Hunan Normal University, Changsha 410081, China*

(Dated: May 31, 2022)

The binary black holes (BBHs) formed near the supermassive black holes (SMBHs) in the galactic nuclei would undergo eccentricity excitation due to the gravitational perturbations from the SMBH and therefore merger more efficiently. In this paper, we study the coupling of the three body 1st post-Newtonian (1pN) effects with the spin effects from the SMBH in the hierarchical triple system. The three body 1pN effects yielding the de-Sitter precession is usually decoupled in the secular dynamics, while it couples to the spin of SMBH through the Lense-Thirring precession of the outer orbital plane. This coupling includes both the precessions of the inner orbit angular momentum and the Runge-Lenz vector around the outer orbit angular momentum in a general reference frame. Our general argument on the coupling of the three body 1pN effects in three body systems could be extended to any other situation as long as the outer orbital plane evolves.

I. INTRODUCTION

The first detection of gravitational wave (GW) from a merger event of a binary black hole (BBH) by LIGO/Virgo[1] in 2015 showed the tremendous success of general relativity (GR) and opened an era of gravitational wave astrophysics. Up to now, the LIGO-VIRGO collaboration observed eleven gravitational wave signals from compact binary mergers during the first and second runs (O1 and O2) [2], and the third observation run (O3) is undergoing since April 2019 [3]. The ground-based detectors mainly focus on the merger and ringdown phase of GW sources which is characterized by a frequency of 10Hz to 1000Hz and a strain of order 10^{-22} , currently we have five of them [4–7].

The space-based detector Laser Interferometer Space Antenna (LISA) is expected to explore the lower frequency GW sources with frequency range 10^{-4} Hz to 1 Hz and characteristic strain of order 10^{-21} [8]. The DECi-hertz Interferometer Gravitational wave Observatory (DECIGO) is aiming to fill the gap between LIGO and LISA with frequency band around 10^{-2} Hz to 10 Hz [9]. There are several other big projects on the space detectors in the future: advanced LISA (aLISA) [10], Tian-Qin and Taiji in China [11, 12]. The space and ground based gravitational wave detectors could cover all the inspiral-merger-ringdown phase of compact binaries. The observations of GWs enable us to figure out the binary

formation channels (see e.g. [13, 14]), test the validity of GR in the strong-field regime (see e.g. [15–17]), and shed light on the gravitational wave astrophysics [18–21].

The origin of the LIGO/Virgo BBHs is a mystery. Conventionally, they are believed to be formed as the remnant of massive binary stars or they are formed dynamically in the star clusters [22]. While according to the recent studies, the centers of galaxies [23], especially those hosting supermassive black holes (SMBHs) [24] are also important places for BBHs to form. In these environments, the merger rate of BBHs could be enhanced to a significant fraction of the LIGO/Virgo event rate due to the complex astrophysical dynamics [25–34]. And a fraction of the BBHs in galaxy centers could either form at [31–33, 35, 36] or be captured to places very close to the SMBHs [37, 38].

The BBH formed near the SMBH composes a stable hierarchical triple system. Here, we call it the "SMBH-BBH" triple system, where the BBH as the inner binary and their center of mass revolving around the SMBH at a larger outer orbit. The BBH is perturbed by the SMBH, and the dominant Newtonian quadrupole perturbation causes the "Kozai-Lidov" oscillation [39–41] on the BBH orbit. The Kozai-Lidov oscillation is described by the exchange between the inner orbital eccentricity and the inclination angle, as a result of the interaction between the inner and the outer orbit angular momentum.

The general relativistic effects are proved to be important in the secular evolution of three body systems. The relativity precession of the inner orbital pericenter is known to suppress the Kozai-Lidov oscillation [41, 42] if the time scale of the former is shorter than the later. And the gravitational radiation is known to circularize

* fangyun@mail.itp.ac.cn

† huangqg@itp.ac.cn

and shrink the binary orbit [42, 43]. These two effects are resulted from binary post-Newtonian (pN) interactions. The three body pN effects come from the interactions between three bodies at pN orders which are considered in [44–47]. Naoz et al. [44] found there is a resonant eccentricity excitation behavior in three body pN dynamics under some parameter space by conducting an orbit-averaged three body 1pN Hamiltonian, though, the Hamiltonian approach dose not resolving the full three body pN effects which is stated in [45, 47]. Will points out that to find the full solution to the problem of secular evolution with quadrupole and 1PN effects together, the cross terms in the aceractions [45] and a multiple-scale analysis to account for the corrections of the periodic effects are needed [46]. When the mass of the inner binary is relatively small, it is found in [47] there are three dominant three body pN effects, where the main effect is the de Sitter precession [54] which comes directly from the accelerations. The above works either consider the three body systems at 1pN order or assume Schwarzschild black holes. In these cases, the outer orbital plane is nearly a constant, while our recent studies [48, 49] show that when it comes to a three body system where the third body is a spinning SMBH, the outer orbital plane will precess due to the spin of the SMBH. As a result, the secular dynamics will depend on the angle between the two orbital line of nodes ($\Omega - \Omega_3$), thus lead to different evolutionary behaviors.

The observations indicate that the SMBHs are universally spinning [50, 51]. We find in [48] the spin effects from the SMBH will modulate the Kozai-Lidov oscillation by causing a Lense-Thirring precession on the outer orbit as well as an another precession on the inner orbit, and derived a generalized Kozai-Lidov formula which could include the evolving outer orbital plane. Afterwards, Liu and Lai [52] noticed that the de-Sitter precession of the inner orbit also becomes important when combined with the Lense-Thirring precession of the outer orbit. However, in Liu and Lai’s consideration, they only added the precession of the inner orbit angular momentum around the outer orbit one which we point out in this work is just a part of the de-Sitter precession in this case.

In this work, we study the secular dynamics of the SMBH-BBH triple systems up to 1.5pN order, especially the coupling of the three body 1pN effects with the spin effects from the SMBH. We resolve the three body 1pN effects start from the Einstein-Infeld-Hoffmann equations of motion [53], which causes the de-Sitter precession on the inner orbit. The de-Sitter precession only has a precession on the inner orbital longitude of ascending node Ω seen from a reference frame set on a constant outer orbital plane, is decoupled in the standard Kozai-Lidov formula where the dependence on Ω is vanished. Since the spin effects from the SMBH would cause the outer orbital plane to precess, the generalized kozai-Lidov formula in this case will depend on the relative angle of nodes ($\Omega - \Omega_3$)[48], thus the de-Sitter precession will be coupled in the secular dynamics. We point out in this

work that this coupling includes both the precession of the inner orbit angular momentum and the Runge-Lenz vector around the outer orbit angular momentum in a general reference frame where the Z axis is not set to the outer orbit angular momentum due to the Lense-Thirring precession. As a whole result, the maximal eccentricity excited by the Kozai-Lidov oscillation is evolving at the Kozai-Lidov timescale due to the change of the vertical inner orbit angular momentum, which is only caused by the spin of the SMBH in our considerations. The characteristics coded in the GWs of BBHs could be potentially used to probe the existence of BBHs near a spinning SMBH, or to probe the spin parameters of SMBHs.

This paper is organized as follows. We calculate the equations of motion in section II. In subsections II A and II B, we analysis the Newtonian quadrupole order, full 1pN order and the 1.5pN order equations of motion. In section III we calculate systematically the three body 1pN order effects in a general reference frame and discuss the connections between the secular equations of motion listed in section II. We present our numerical results in section IV. In subsection IV A, we show numerical results of the general relativity effects calculated and considered in this work. And in subsection IV B, we show typical characteristics on GW singles due to spin effects. We conclude our paper in section V.

Throughout this paper we use the natural units with $c = G = 1$ in our calculations.

II. EQUATIONS OF MOTION UP TO 1.5PN ORDER

A. Full 1pN dynamics

We now consider a hierarchical three-body system in which the binary bodies of mass m_1 and m_2 are in a close orbit with separation r , their center of mass revolving around a SMBH of mass m_3 at a much larger distance $R(\gg r)$. We define the relative separation vector of the binary system and the vector from the center of mass of the binary to the SMBH by

$$\mathbf{x} \equiv \mathbf{x}_1 - \mathbf{x}_2, \quad \mathbf{X} \equiv \mathbf{x}_3 - \mathbf{x}_0, \quad (1)$$

where

$$\mathbf{x}_0 \equiv \frac{m_1 \mathbf{x}_1 + m_2 \mathbf{x}_2}{m}, \quad (2)$$

is the center of mass of the inner binary, and $m \equiv m_1 + m_2$. We work in the center of mass-frame of the entire system, thus,

$$m_1 \mathbf{x}_1 + m_2 \mathbf{x}_2 + m_3 \mathbf{x}_3 = m \mathbf{x}_0 + m_3 \mathbf{x}_3 = 0, \quad (3)$$

where we have ignored the post-Newtonian corrections to the center of mass. Then, the positions of the three bodies are,

$$\mathbf{x}_1 = \frac{m_2}{m} \mathbf{x} + \frac{m_3}{M} \mathbf{X}, \quad \mathbf{x}_2 = -\frac{m_1}{m} \mathbf{x} + \frac{m_3}{M} \mathbf{X}, \quad \mathbf{x}_3 = -\frac{m}{M} \mathbf{X}, \quad (4)$$

where $M = m_1 + m_2 + m_3$ is the total mass. Since the mass of SMBH is much larger than the binary system, with $m_3 \gg m$, the center of mass frame of the entire system is set to the position of m_3 . Thus Eq. (4) is simplified to

$$\mathbf{x}_1 = \frac{m_2}{m} \mathbf{x} + \mathbf{X}, \quad \mathbf{x}_2 = -\frac{m_1}{m} \mathbf{x} + \mathbf{X}, \quad \mathbf{x}_3 = 0, \quad (5)$$

We also define the velocities $\mathbf{v} \equiv d\mathbf{x}/dt$, $\mathbf{V} \equiv d\mathbf{X}/dt$, accelerations $\mathbf{a} \equiv d\mathbf{v}/dt$, $\mathbf{A} \equiv d\mathbf{V}/dt$, distances $r \equiv |\mathbf{x}|$, $R \equiv |\mathbf{X}|$, and unit vectors $\mathbf{n} \equiv \mathbf{x}/r$, $\mathbf{N} \equiv \mathbf{X}/R$.

The accelerations are directly computed with the post-Newtonian N-body equations of motion, which is commonly referred to as the Einstein-Infeld-Hoffman equations of motion [53]:

$$\begin{aligned} \mathbf{a}_a = & -\sum_{b \neq a} \frac{m_b \mathbf{x}_{ab}}{r_{ab}^3} \\ & + \sum_{b \neq a} \frac{m_b \mathbf{x}_{ab}}{r_{ab}^3} \left[4 \frac{m_b}{r_{ab}} + 5 \frac{m_a}{r_{ab}} + \sum_{c \neq a, b} \frac{m_c}{r_{bc}} + 4 \sum_{c \neq a, b} \frac{m_c}{r_{ac}} \right. \\ & \left. - \frac{1}{2} \sum_{c \neq a, b} \frac{m_c}{r_{bc}^3} (\mathbf{x}_{ab} \cdot \mathbf{x}_{bc}) - v_a^2 + 4\mathbf{v}_a \cdot \mathbf{v}_b - 2v_b^2 + \frac{3}{2} (\mathbf{v}_b \cdot \mathbf{n}_{ab})^2 \right] \\ & - \frac{7}{2} \sum_{b \neq a} \frac{m_b}{r_{ab}} \sum_{c \neq a, b} \frac{m_c \mathbf{x}_{bc}}{r_{bc}^3} + \sum_{b \neq a} \frac{m_b}{r_{ab}^3} \mathbf{x}_{ab} \cdot (4\mathbf{v}_a - 3\mathbf{v}_b)(\mathbf{v}_a - \mathbf{v}_b), \end{aligned} \quad (6)$$

where $r_{ab} = |\mathbf{x}_{ab}| = |\mathbf{x}_a - \mathbf{x}_b|$, $\mathbf{n}_{ab} = \mathbf{x}_{ab}/r_{ab}$, $\mathbf{v}_a = d\mathbf{x}_a/dt$, and a, b, c denotes 1, 2, 3.

The inner binary acceleration could be decomposed as follows,

$$\begin{aligned} \mathbf{a} = & -\frac{m\mathbf{n}}{r^2} - \frac{m_3 r}{R^3} [\mathbf{n} - 3(\mathbf{n} \cdot \mathbf{N})\mathbf{N}] + [\mathbf{a}]_{\text{binary1pN}} \\ & + [\mathbf{a}]_{\text{3body1pN}} + O\left(\frac{mm_3}{R^3}\right) + O\left(\frac{m_3^2 r}{R^4}\right) + O\left(\frac{m^2 r}{r^3 R}\right) + \dots, \end{aligned} \quad (7)$$

where we have expanded the Newtonian perturbation term from the third body to quadrupole order. And $[\mathbf{a}]_{\text{binary1pN}}$ is the 1pN order acceleration of the binary system (m_1 and m_2), while $[\mathbf{a}]_{\text{3body1pN}}$ is the 1pN order acceleration contribute by the three body interactions. To leading order, they are

$$[\mathbf{a}]_{\text{binary1pN}} = \frac{m\mathbf{n}}{r^2} \left[(4 + 2\eta) \frac{m}{r} - (1 + 3\eta)v^2 + \frac{3}{2} \eta (\mathbf{n} \cdot \mathbf{v})^2 \right] + (4 - 2\eta) \frac{m(\mathbf{n} \cdot \mathbf{v})\mathbf{v}}{r^2}, \quad (8)$$

$$\begin{aligned} [\mathbf{a}]_{\text{3body1pN}} = & \frac{5mm_3\mathbf{n}}{r^2 R} + \frac{m}{r^2} \left\{ \left[\frac{3}{2} (\mathbf{n} \cdot \mathbf{V})^2 - 2\Delta \mathbf{v} \cdot \mathbf{V} + V^2 \right] \mathbf{n} - \Delta (\mathbf{n} \cdot \mathbf{V}) \mathbf{v} \right\} \\ & + \frac{m_3}{R^2} [4\mathbf{v} \cdot \mathbf{N} (\mathbf{V} - \Delta \mathbf{v}) + (\Delta v^2 - 2\mathbf{v} \cdot \mathbf{V})\mathbf{N} + 4(\mathbf{V} \cdot \mathbf{N})\mathbf{v}] \\ & + \frac{\Delta mm_3}{2rR^2} [9(\mathbf{n} \cdot \mathbf{N})\mathbf{n} - \mathbf{N}], \end{aligned} \quad (9)$$

where $\eta = \frac{m_1 m_2}{m^2}$, $\Delta = \frac{m_1 - m_2}{m}$. We only keep the dominant terms in $[\mathbf{a}]_{\text{3body1pN}}$ which are combined of $\frac{m}{r^2}$ or $\frac{m_3}{R^2}$ with $v^2 (\sim \frac{m}{r})$, $V^2 (\sim \frac{m_3}{R})$, or $\mathbf{v} \cdot \mathbf{V}$.

We treat the acceleration of the outer binary as the similar way:

$$\begin{aligned} \mathbf{A} = & -\frac{M\mathbf{N}}{R^2} + \frac{3}{2} \frac{M\eta r^2}{R^4} [\mathbf{N} (1 - 5(\mathbf{n} \cdot \mathbf{N})^2) + 2\mathbf{n}(\mathbf{n} \cdot \mathbf{N})] + [\mathbf{A}]_{\text{binary1pN}} \\ & + [\mathbf{A}]_{\text{3body1pN}} + O\left(\frac{mm_3}{R^3}\right) + O\left(\frac{m_3^2 r}{R^4}\right) + O\left(\frac{m^2 r}{r^3 R}\right) + \dots, \end{aligned} \quad (10)$$

where

$$[\mathbf{A}]_{\text{binary1pN}} = \frac{m_3 \mathbf{N}}{R^2} \left(\frac{4m_3}{R} - V^2 \right) + \frac{4m_3}{R^2} (\mathbf{V} \cdot \mathbf{N}) \mathbf{V}, \quad (11)$$

$$[\mathbf{A}]_{\text{3body1pN}} = \frac{\eta m \mathbf{n}}{r^2} \left\{ \frac{\Delta m}{r} - 3(\mathbf{n} \cdot \mathbf{v})(\mathbf{n} \cdot \mathbf{V}) + \Delta \left[\frac{3}{2} (\mathbf{n} \cdot \mathbf{v})^2 - v^2 \right] + 2\mathbf{v} \cdot \mathbf{V} \right\}$$

$$\begin{aligned}
& + \frac{\eta m \mathbf{v}}{r^2} (2 \mathbf{n} \cdot \mathbf{V} - \Delta \mathbf{n} \cdot \mathbf{v}) + \frac{\eta m_3}{R^2} [4(\mathbf{v} \cdot \mathbf{N})\mathbf{v} - v^2 \mathbf{N}] \\
& + \frac{\eta m m_3}{r R^2} [\mathbf{N} - 4(\mathbf{n} \cdot \mathbf{N})\mathbf{n}], \tag{12}
\end{aligned}$$

The first terms in Eq. (7) and (10) are the leading Newtonian gravitational force which form the Kepler orbit of the inner and outer binary, and the rests in Eqs. (7) and (10) are all treated as perturbations. The second terms are the Newtonian quadrupole forces which cause the Kozai-Lidov oscillation [55]. The binary 1pN acceleration contains the standard terms for a body in orbit around a point mass m (or m_3). The three body 1pN accelerations comes from the leading three body interactions at 1pN which results the de-Sitter precession as will be seen in the section III.

B. 1.5 pN dynamics from the spin of the SMBH

In the previous paper [48, 49], we studied the spin effects from the SMBH on the dynamical evolution of a nearby BBH. In the SMBH-BBH triple system, the gravitational potential is dominated by the mass of the SMBH which contributes the electrical part of dynamics. And similarly, for a relatively large spin parameter of the SMBH, its spin angular momentum will dominant the total angular momentum of this system which contributes the magnetical part of the dynamics [48, 49, 56]. The spin of the SMBH will induce a strong gravitomagnetic field (denoted as \mathcal{H}) in its spacetime. The BBH move close to the rotating SMBH will feel the gravitomagnetic force $\mathbf{v}_a \times \mathcal{H}$ [56, 57], and the field \mathcal{H} is related to the spin momentum \mathbf{S} as

$$\mathcal{H} = \nabla \times \left(-2 \frac{\mathbf{S} \times \mathbf{r}}{r^3} \right), \tag{13}$$

where $\mathbf{S} = a m_3 \mathbf{s}$, a/m_3 is the dimensionless spin parameter, \mathbf{s} is the spin direction vector, and \mathbf{r} here denote a general direction of position.

Decomposing the gravitomagnetic force into the inner and outer orbit equation of motion, the accelerations are dominated by [48]

$$\mathbf{a}_{[1.5\text{PN}, \text{spin}]} \simeq 2a m_3 \mathbf{v} \times \frac{(\mathbf{e}_z - 3(\mathbf{e}_z \cdot \mathbf{N})\mathbf{N})}{R^3}, \tag{14}$$

$$\mathbf{A}_{[1.5\text{PN}, \text{spin}]} \simeq 2a m_3 \mathbf{V} \times \frac{(\mathbf{e}_z - 3(\mathbf{e}_z \cdot \mathbf{N})\mathbf{N})}{R^3}, \tag{15}$$

The force in (15) causes the Lense-Thirring precession of the out orbit while the force in (14) causes another precession on the inner orbit which is listed in the next section.

III. SECULAR EVOLUTION OF THE ORBIT ELEMENTS

We are interested in the secular evolutions which are left after a complete evolution of the inner and outer orbit. This is obtained by average the Lagrange planetary equations over the period of the inner and outer orbital (see e.g. [58]). We denote the inner and outer orbits with the time-dependent osculating orbital elements $\{p, e, \omega, \Omega, \iota\}$ and $\{P, E, \omega_3, \Omega_3, \iota_3\}$ respectively. See Fig. 1 for details. The positions and velocities of each orbit are defined in terms of the orbital elements as

$$\begin{aligned}
\mathbf{r} &= p \mathbf{n} / (1 + e \cos f), \\
\mathbf{v} &= \sqrt{\frac{m}{p}} \left[e \sin f \mathbf{n} + (1 + e \cos f) \boldsymbol{\lambda} \right], \\
\mathbf{R} &= P \mathbf{N} / (1 + E \cos F), \\
\mathbf{V} &= \sqrt{\frac{M}{P}} \left[E \sin F \mathbf{N} + (1 + E \cos F) \boldsymbol{\Lambda} \right], \tag{16}
\end{aligned}$$

where the bases $(\mathbf{n}, \boldsymbol{\lambda}, \mathbf{h})$ and $(\mathbf{N}, \boldsymbol{\Lambda}, \mathbf{H})$ are defined on the inner and outer orbital plane which are related to the reference frame $(\mathbf{e}_X, \mathbf{e}_Y, \mathbf{e}_Z)$ by Euler angles [58]:

$$\begin{aligned}
\mathbf{n} &= [\cos \Omega \cos(\omega + \phi) - \cos \iota \sin \Omega \sin(\omega + \phi)] \mathbf{e}_X \\
&+ [\sin \Omega \cos(\omega + \phi) + \cos \iota \cos \Omega \sin(\omega + \phi)] \mathbf{e}_Y \\
&+ \sin \iota \sin(\omega + \phi) \mathbf{e}_Z, \\
\boldsymbol{\lambda} &= \frac{d\mathbf{n}}{d\phi}, \quad \mathbf{h} = \mathbf{n} \times \boldsymbol{\lambda}, \tag{17}
\end{aligned}$$

$$\begin{aligned}
\mathbf{N} &= [\cos \Omega_3 \cos(\omega_3 + \Phi) - \cos \iota_3 \sin \Omega_3 \sin(\omega_3 + \Phi)] \mathbf{e}_X \\
&+ [\sin \Omega_3 \cos(\omega_3 + \Phi) + \cos \iota_3 \cos \Omega_3 \sin(\omega_3 + \Phi)] \mathbf{e}_Y \\
&+ \sin \iota_3 \sin(\omega_3 + \Phi) \mathbf{e}_Z,
\end{aligned}$$

$$\boldsymbol{\Lambda} = \frac{d\mathbf{N}}{d\Phi}, \quad \mathbf{H} = \mathbf{N} \times \boldsymbol{\Lambda}. \tag{18}$$

And the semi-major axis for the inner and outer orbits are respectively $\alpha = p(1 - e^2)$ and $\mathcal{A} = P(1 - E^2)$.

We define the perturbing accelerations as $\delta \mathbf{a} = \mathbf{a} + \frac{m_3}{r^2} \mathbf{n}$ and $\delta \mathbf{A} = \mathbf{A} + \frac{m_3}{R^2} \mathbf{N}$. The orbits are perturbed from Kepler orbit. Take the the inner orbit for example, the equation of motion is govern by

$$\frac{d\mathbf{h}}{dt} = \mathbf{r} \times \delta \mathbf{a}, \quad m \frac{d\mathbf{Q}}{dt} = \delta \mathbf{a} \times \mathbf{h} + \mathbf{v} \times (\mathbf{r} \times \delta \mathbf{a}), \tag{19}$$

where $\mathbf{h} \equiv \mathbf{r} \times \mathbf{v} = \sqrt{m p} \mathbf{h}$, and \mathbf{Q} is the Runge-Lenz vector which is defined by $\mathbf{Q} \equiv \mathbf{v} \times \mathbf{h} / m - \mathbf{n} = e(\cos \phi \mathbf{n} - \sin \phi \boldsymbol{\lambda})$.

The equations of motion of orbital elements are obtained by resolving the equations in (19) as,

$$\frac{dp}{dt} = 2 \sqrt{\frac{p^3}{m}} \frac{\mathcal{S}}{1 + e \cos \phi},$$

$$\begin{aligned}
\frac{d\iota_3}{d\tau} &= -\frac{3\pi\alpha^{7/2}m_1m_2\sqrt{M}}{4\mathcal{A}^{7/2}(1-E^2)^2m^{5/2}} \left(\cos\iota_3 \left\{ \sin 2\iota \sin(\Omega - \Omega_3)(-5e^2 \cos^2 \omega + 4e^2 + 1) - 5e^2 \sin \iota \sin 2\omega \cos(\Omega - \Omega_3) \right\} \right. \\
&\quad \left. + \sin\iota_3 \left\{ \sin(2\Omega - 2\Omega_3) [\sin^2 \iota(-5e^2 \cos^2 \omega + 4e^2 + 1) + 10e^2 \cos^2 \omega - 5e^2] + 5e^2 \cos \iota \sin 2\omega \cos(2\Omega - 2\Omega_3) \right\} \right), \\
\frac{d\Omega_3}{d\tau} &= -\frac{3\pi\alpha^{7/2}m_1m_2\sqrt{M} \csc \iota_3}{8\mathcal{A}^{7/2}(1-E^2)^2m^{5/2}} \left(\cos 2\iota_3 \left\{ \sin 2\iota \cos(\Omega - \Omega_3)(5e^2 \cos 2\omega - 3e^2 - 2) - 10e^2 \sin \iota \sin 2\omega \sin(\Omega - \Omega_3) \right\} \right. \\
&\quad \left. + \sin 2\iota_3 \left\{ \frac{1}{2} \sin^2 \iota [\cos(2\Omega - 2\Omega_3) + 3] (5e^2 \cos 2\omega - 3e^2 - 2) + 5e^2 \cos \iota \sin 2\omega \sin(2\Omega - 2\Omega_3) \right. \right. \\
&\quad \left. \left. - 5e^2 \cos 2\omega \cos(2\Omega - 2\Omega_3) + 3e^2 + 2 \right\} \right), \\
\frac{d\varpi_3}{d\tau} &= \frac{3\pi\alpha^{7/2}m_1m_2\sqrt{M}}{16\mathcal{A}^{7/2}(1-E^2)^2m^{5/2}} \left(30e^2 \sin \iota \sin 2\iota_3 \sin 2\omega \sin(\Omega - \Omega_3) - 30e^2 \sin^2 \iota_3 \cos \iota \sin 2\omega \sin(2\Omega - 2\Omega_3) \right. \\
&\quad \left. + 3 \sin^2 \iota_3 \cos(2\Omega - 2\Omega_3) [\sin^2 \iota(-5e^2 \cos 2\omega + 3e^2 + 2) + 10e^2 \cos 2\omega] \right. \\
&\quad \left. + 3 \sin 2\iota \sin 2\iota_3 \cos(\Omega - \Omega_3)(-5e^2 \cos 2\omega + 3e^2 + 2) + (2 - 3 \sin^2 \iota_3) [\sin^2 \iota(15e^2 \cos 2\omega - 9e^2 - 6) + 6e^2 + 4] \right), \tag{23}
\end{aligned}$$

where the time derivation d/dt is converted to a dimensionless one $d/d\tau$ by rescaling time compared to the inner orbital period with $\tau \equiv t/T_{\text{in}} = \frac{t}{2\pi} \sqrt{\frac{m}{\alpha^3}}$.

If the outer orbital plane is nearly a constant, then the reference frame could be set approximately on the orbital plane where \mathbf{J}_{out} is depart from Z axis by a very small angle $\iota_3 \rightarrow 0$. Then we could expand the expressions in Eq. (23) by ι_3 as

$$\begin{aligned}
\frac{de}{d\tau} &= \frac{15\pi}{2} \frac{\alpha^3 m_3 e (1-e^2)^{1/2}}{\mathcal{A}^3 m (1-E^2)^{3/2}} \sin^2(\iota + \iota_3) \sin \omega \cos \omega + O(\iota_3), \\
\frac{d\iota}{d\tau} &= -\frac{15\pi}{4} \frac{\alpha^3 m_3 e^2}{\mathcal{A}^3 m (1-e^2)^{1/2} (1-E^2)^{3/2}} \sin 2(\iota + \iota_3) \sin \omega \cos \omega + O(\iota_3), \\
\frac{d\Omega}{d\tau} &= -\frac{3\pi}{4} \frac{\alpha^3 m_3}{\mathcal{A}^3 m (1-e^2)^{1/2} (1-E^2)^{3/2}} \frac{\sin 2(\iota + \iota_3)}{\sin \iota} (1 + 4e^2 - 5e^2 \cos^2 \omega) + O(\iota_3), \\
\frac{d\varpi}{d\tau} &= \frac{3\pi}{2} \frac{\alpha^3 m_3 (1-e^2)^{1/2}}{\mathcal{A}^3 m (1-E^2)^{3/2}} [1 - \sin^2(\iota + \iota_3)(4 - 5 \cos^2 \omega)] + O(\iota_3), \\
\frac{dE}{d\tau} &= 0, \\
\frac{d\iota_3}{d\tau} &= -\frac{15\pi}{2} \frac{\alpha^{7/2} m_1 m_2 \sqrt{M} e^2}{\mathcal{A}^{7/2} m^{5/2} (1-E^2)^2} \sin(\iota + \iota_3) \sin \omega \cos \omega + O(\iota_3), \\
\frac{d\Omega_3}{d\tau} &= -\frac{3\pi}{4} \frac{\alpha^{7/2} m_1 m_2 \sqrt{M}}{\mathcal{A}^{7/2} m^{5/2} (1-E^2)^2} \frac{\sin 2(\iota + \iota_3)}{\sin \iota_3} (1 + 4e^2 - 5e^2 \cos^2 \omega) + O(\iota_3), \\
\frac{d\varpi_3}{d\tau} &= \frac{3\pi}{4} \frac{\alpha^{7/2} m_1 m_2 \sqrt{M}}{\mathcal{A}^{7/2} m^{5/2} (1-E^2)^2} [2 + 3e^2 - 3 \sin^2(\iota + \iota_3)(1 + 4e^2 - 5e^2 \cos^2 \omega)] + O(\iota_3). \tag{24}
\end{aligned}$$

Where we obtain the standard Kozai-Lidov formula (see e.g. [41, 55]) in the dominant terms of Eq. (24), and the dependence on $\Omega - \Omega_3$ is of order $O(\iota_3)$ smaller than the dominant terms. This means when the outer orbital plane do not change significantly, we could safely use the standard Kozai-Lidov formula to describe the Newtonian quadrupole perturbations. While when the outer orbital plane changes moderately, the secular dynamics will depend on the angle $\Omega - \Omega_3$, and in this case we have to use the Kozai-Lidov formula in the generalized form (23).

The equations in (23) seems a bit more complex compared to the standard Kozai-Lidov formula. But it is a more general description of the Newtonian quadrupole perturbation which could be extended to the case where the outer orbital angular momentum is evolving. And

the generalized Kozai-Lidov formula in Eq. (23) will certainly degenerate to the standard Kozai-Lidov oscillation dynamically with an approximately constant outer orbital plane, as it is guaranteed by the equations of motion. This degeneration happens in two situations. On

the one hand, up to Newtonian order, the total orbital angular momentum of the three body system is strictly conserved. This conservation could simplify the formula in Eq. (23) by the fact that the relation $\Omega - \Omega_3 = \pi$ is precisely granted [55]. On the other hand, if the other orders of perturbations do not change the outer orbital plane, like the de-Sitter precession (as shows in the next part of this section), the dynamics on $\Omega - \Omega_3$ is decoupled with the Newtonian quadrupole perturbations. An analogous discussion also suits the other orders of Newtonian perturbations, like the octupole [59] and the hexadecapole order perturbations [55].

The binary 1pN acceleration in Eqs. (8) and (11) induce the typical relativity precession on the pericenter ω (ω_3) of the binary system by

$$\frac{d\omega}{d\tau} = \frac{6\pi m}{p}, \quad \frac{d\omega_3}{d\tau} = \frac{6\pi M}{P}. \quad (25)$$

In this paper, we derive the secular evolutions contributed by the leading three body 1pN accelerations in our system as presented in Eqs. (9) and (12), the results are listed as bellow,

Leading three body 1pN effects

$$\begin{aligned} \frac{de}{dt} &= \frac{dp}{dt} = 0, \\ \frac{d\iota}{dt} &= -\frac{3m_3^{3/2}}{2\mathcal{A}^{5/2}(1-E^2)} \sin \iota_3 \sin(\Omega - \Omega_3), \\ \frac{d\Omega}{dt} &= \frac{3m_3^{3/2}}{2\mathcal{A}^{5/2}(1-E^2)} [\cos \iota_3 - \sin \iota_3 \cot \iota \cos(\Omega - \Omega_3)], \\ \frac{d\omega}{dt} &= \frac{3m_3^{3/2}}{2\mathcal{A}^{5/2}(1-E^2)} \sin \iota_3 \csc \iota \cos(\Omega - \Omega_3), \\ \frac{dE}{dt} &= \frac{dP}{dt} = \frac{d\iota_3}{dt} = \frac{d\Omega_3}{dt} = \frac{d\omega_3}{dt} = 0, \end{aligned} \quad (26)$$

when \mathbf{J}_{out} depart from Z axis by a very small angle, $\iota_3 \rightarrow 0$, the non-vanishing equations above are expanded as

$$\begin{aligned} \frac{d\Omega}{dt} &= \frac{3m_3^{3/2}}{2\mathcal{A}^{5/2}(1-E^2)} + O(\iota_3), \\ \frac{d\iota}{dt} &= O(\iota_3), \quad \frac{d\omega}{dt} = O(\iota_3), \end{aligned} \quad (27)$$

the precession on ι and Ω in Eq. (26) gives the precession of \mathbf{J}_{in} alone \mathbf{J}_{out} in the de-Sitter precession with an arbitrary direction of \mathbf{J}_{out} . And the precession on Ω in Eq. (27) gives the de-Sitter precession when \mathbf{J}_{out} is fixed and set in Z axis. In Eq. (26), there is an extra precession on ω which seems weird compared to (27) superficially, which turns out to be the precession of the Runge-Lenz vector \mathbf{Q} alone the direction of \mathbf{J}_{out} as a part of de-Sitter precession in the general reference frame. The angle ω is not precessing in de-Sitter precession when seeing from the outer orbital plane, while it is precessing (alone \mathbf{J}_{out}) from a general reference frame. And for an evolving outer

orbital plane, this ‘‘extra’’ precession on the inner orbital pericenter ω is of the same order as the de-Sitter precession on ι and Ω , and the binary relativity precession in Eq. (25) (under some parameter space), which is not ignorable.

The secular dynamics from the spin effects of the SMBH is resulted by accelerations in (14) and (15), which are calculated in [48]. The non-vanishing results are,

spin effects at 1.5pN order

$$\begin{aligned} \frac{d\iota}{dt} &= \frac{3am_3}{4\mathcal{A}^3(1-E^2)^{3/2}} \sin 2\iota_3 \sin(\Omega - \Omega_3), \\ \frac{d\Omega}{dt} &= -\frac{am_3}{4\mathcal{A}^3(1-E^2)^{3/2}} \\ &\quad \times [-3 \sin 2\iota_3 \cot \iota \cos(\Omega - \Omega_3) + 3 \cos 2\iota_3 + 1], \\ \frac{d\omega}{dt} &= -\frac{3am_3}{4\mathcal{A}^3(1-E^2)^{3/2}} \sin 2\iota_3 \csc \iota \cos(\Omega - \Omega_3), \\ \frac{d\Omega_3}{dt} &= \frac{2am_3}{\mathcal{A}^3(1-E^2)^{3/2}}, \\ \frac{d\omega_3}{dt} &= -\frac{6am_3}{\mathcal{A}^3(1-E^2)^{3/2}} \cos \iota_3, \end{aligned} \quad (28)$$

where the change of Ω_3 in Eq. (28) is the Lense-Thirring precession on the outer orbit. The inner orbit is not simply precessing around the spin axis, but it is precessing in a rather complex way. Note that up to the orders considered in our full text, the outer orbital pericenter ω_3 is decoupled from the evolution of other orbital elements.

IV. NUMERICAL RESULTS

A. On the dynamical evolution

In this subsection, we display the numerical results of our SMBH-BBH three body system. We begin with a group of initial data with a BBH of mass $m_1 = 20M_\odot$ and $m_2 = 20M_\odot$, which are the typical mass detected by LIGO/Virgo. The third body is a SMBH with $m_3 = 4 \times 10^6 M_\odot$ which is similar to the one in our galaxy center. The inner binary is separated with semi-major axis $\alpha = 0.04$ AU and has an initial eccentricity $e = 0.1$. They are set to a distance of $\mathcal{A} = 30$ AU to the SMBH with an outer orbit eccentricity $E = 0.1$. The line of apsides of the two orbits are set to X axis thus $\Omega = \Omega_3 = \omega = \omega_3 = 0$, and the inclination angle between the two orbits is simply $\iota - \iota_3$ for convenience but not lose generality.

In Fig. 2, we display the numerical evolution of eccentricity. In the red line, we have included all the dynamical effects considered in this work, with the Newtonian quadrupole effect (Kozai-Lidov) in Eq. (23), the binary 1pN precession in Eq. (25), the three body 1pN effects in Eq. (26), the spin effects in Eq. (28), and redaction reaction [43]. The dashed blue line has the same initial data with the red line except that it lacks the three body 1pN effects in Eq. (26). We could see in Fig. 2 these two

lines are significantly different, which indicates the three body 1pN effects (de-Sitter precession) is coupled in the secular dynamics with the Lense-Thirring precession on the outer orbit.

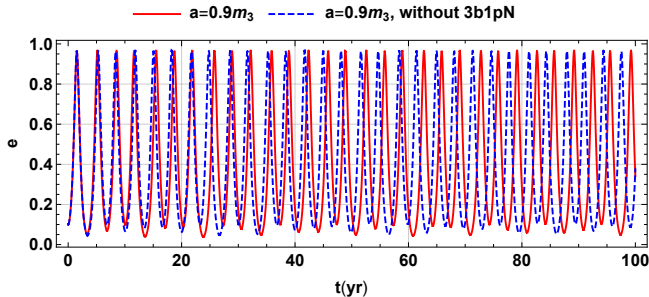


FIG. 2. The evolution of eccentricity in 100 years. The initial conditions of the two lines are: $\iota_3 = 60^\circ$ and $\iota = 140^\circ$, thus the initial angle between \mathbf{J}_{in} and \mathbf{J}_{out} is $\iota - \iota_3 = 80^\circ$, and the SMBH has a spin parameter of $a = 0.9m_3$. The red line has included all the dynamical effects considered in this work, while the dashed blue line only lacks the three body 1pN effects (denoted as 3b1pN in the figure) in Eq. (26) compared to the red line.

As a comparison, it is trivial to verify that the de-Sitter precession decouples when the Lense-Thirring precession disappears when $a = 0$ or initially $\iota_3 = 0$.

B. On the gravitational waves

The maximal eccentricity of the inner orbit excited by the Kozai-Lidov oscillation is limited to the vertical inner orbit angular momentum (which is proportional to $\Theta = \sqrt{1 - e^2} \mathbf{h} \cdot \mathbf{H}$) as [41, 60]:

$$e_{\text{max}} = \sqrt{1 - \frac{5}{3} \Theta^2}. \quad (29)$$

Since the de-Sitter precession do not change the value of Θ , here it changes only due to the spin of the SMBH, by

$$\Theta'(t) = \frac{3\sqrt{1 - e^2} (\mathbf{S} \times \mathbf{H}) \cdot \mathbf{h}}{2\mathcal{A}^3 (1 - E^2)^{3/2}}, \quad (30)$$

where \mathbf{S} is the spin angular momentum, \mathbf{h} and \mathbf{H} are the unit direction of \mathbf{J}_{in} and \mathbf{J}_{out} respectively as discussed before. And the peak frequency of GW is closely related to eccentricity by $f_{\text{peak}} = \frac{\sqrt{m}(1+e)^{-0.3046}}{\pi[\alpha(1-e)]^{3/2}}$ [42]. We plot the evolution of eccentricity near its maximal values in the upper panel of Fig. 2, and the corresponding peak frequency f_{peak} in the lower panel. It could be seen that the maximal eccentricity is evolving at the Kozai-Lidov timescale when the SMBH is spinning (the red line) while it remains constant in the case without spin (the dashed black line). Thus, the closest pericenter $(1 - e_{\text{max}})\alpha$ in the neighboring Kozai-Lidov circles could be different by several percent in this example. As a result, the difference

of the maximal values of f_{peak} in the neighboring Kozai-Lidov circles could reach to nearly 0.001Hz as shows in the lower panel.

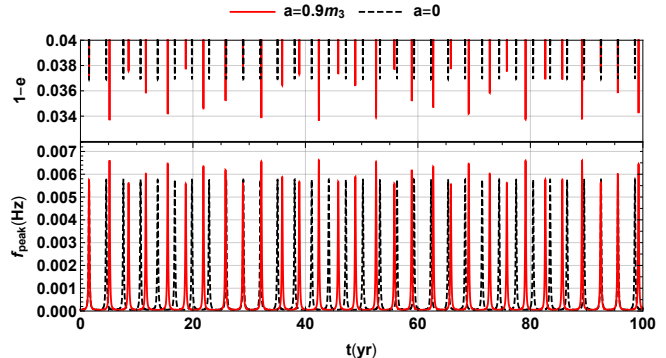


FIG. 3. Upper panel: zoom in of the evolution of eccentricity near its maximal values. Lower panel: the peak frequency of the GWs correspond to the eccentricity in the upper panel. The red lines have the same line styles with that in Fig. 2, while the dashed black line is only different from the red line by the spin parameter of the SMBH with $a = 0$.

Interestingly, when the eccentricity of the BBH is excited to a relatively large number, the peak frequency of GWs could locate in LISA band as can be seen in Fig. 3. The different behaviors on the values of e_{max} and/or f_{peak} in different Kozai-Lidov cycles might be important characteristics to prob the spin effects of SMBH. We have discussed in the work [49] that the GW singles from the BBH could be potentially used to probe the spin of the SMBH. Here, we step this topic a little further by stating the unique characteristics due to the spin effects on the GWs.

V. CONCLUSION

In this work, we solve the secular evolution of the three body system which composing a BBH and a spinning SMBH up to 1.5pN at the leading order. The spin effects from the SMBH will modulate the Kozai-Lidov effects by causing the Lense-Thirring precession on the outer orbit and an extra precession on the inner orbit as was found in our previous work [48]. In this work, we study the coupling of the three body 1pN effects with the spin effects from the SMBH, by resolving the Einstein-Infeld-Hoffmann equations of motion. We conduct the double average of the Lagrange planetary equations to get the secular evolutionary equations with the help of Mathematica software.

The three body 1pN effects lead to the de-Sitter precession on the inner orbit is decoupled in the secular dynamics with a constant outer orbital plane. While in our triple system, the spin effects from the SMBH will cause the outer orbital plane to precession (Lense-Thirring precession), thus the Kozai-Lidov formula has to be extended to the generalized form [48] which depends

on the the angle between the two lines of nodes $\Omega - \Omega_3$. Therefore, the de-Sitter precession will be coupled in the secular dynamics by causing both the precession of the inner orbit angular momentum and the Runge-Lenz vector around the outer orbit angular momentum in a general reference frame where the Z axis is not set to the outer orbit angular momentum. Our general argument on the coupling of the three body 1pN effects could be extended to any situation where the outer orbital plane is evolving due to other mechanisms, such as a non-spherical gravitational potential [61, 62].

We also point out that the maximal eccentricity excited by the Kozai-Lidov oscillation is evolving at the Kozai-Lidov timescale due to the change of the vertical inner orbit angular momentum, which is only caused by the spin effects from the SMBH in our context. As a result, the maximal peak frequency of the GWs emitted by the BBH is different in the neighboring Kozai-Lidov circles. Interestingly, when the maximal eccentricity of the

BBH is excited to a relatively large number under some space of parameters, the peak frequency of gravitational wave could locate in LISA band. In our numerical example, the peak frequency of GW locates in LISA band, and the difference of the maximal peak frequency in the neighboring Kozai-Lidov circles could reach to a value of nearly 0.001Hz. It indicates the characteristics in the GW singles from the BBH could be potentially be used to probe the existence of BBH near a spinning SMBH, or could be potentially used to prob the spin of the SMBH as is discussed in [49]. The details about the detectable space of parameters and methods are left to future works.

Acknowledgments. We would like to thank Xian Chen and Misao Sasaki for useful discussions. This work is supported by grants from NSFC (grant No. 11975019, 11690021, 11991053, 11947302), the Strategic Priority Research Program of Chinese Academy of Sciences (Grant No. XDB23000000, XDA15020701), and Key Research Program of Frontier Sciences, CAS, Grant NO. ZDBS-LY-7009.

-
- [1] B. P. Abbott *et al.* (LIGO Scientific, Virgo), *Phys. Rev. Lett.* **116**, 061102 (2016), arXiv:1602.03837 [gr-qc].
- [2] B. P. Abbott *et al.* (LIGO Scientific, Virgo), *Phys. Rev. X* **9**, 031040 (2019), arXiv:1811.12907 [astro-ph.HE].
- [3] “Gravitational-wave candidate event database,” <https://gracedb.ligo.org/latest/>.
- [4] “Ligo,” <https://www.ligo.caltech.edu/>.
- [5] “Virgo,” <http://www.virgo-gw.eu/>.
- [6] “Kagra,” <https://gwcenter.icrr.u-tokyo.ac.jp/en/archives/1381>.
- [7] “Geo600,” <https://www.geo600.org/>.
- [8] P. A. Seoane *et al.* (eLISA), (2013), arXiv:1305.5720 [astro-ph.CO].
- [9] S. Sato *et al.*, *Proceedings, 11th International LISA Symposium: Zurich, Switzerland, September 5-9, 2016*, *J. Phys. Conf. Ser.* **840**, 012010 (2017).
- [10] “advanced lisa,” <http://www.srl.caltech.edu/~shane/sensitivity/>.
- [11] J. Luo *et al.* (TianQin), *Class. Quant. Grav.* **33**, 035010 (2016), arXiv:1512.02076 [astro-ph.IM].
- [12] W.-H. Ruan, Z.-K. Guo, R.-G. Cai, and Y.-Z. Zhang, (2018), arXiv:1807.09495 [gr-qc].
- [13] K. Breivik, C. L. Rodriguez, S. L. Larson, V. Kalogera, and F. A. Rasio, *Astrophys. J.* **830**, L18 (2016), arXiv:1606.09558 [astro-ph.GA].
- [14] C. L. Rodriguez, M. Zevin, C. Pankow, V. Kalogera, and F. A. Rasio, *Astrophys. J.* **832**, L2 (2016), arXiv:1609.05916 [astro-ph.HE].
- [15] E. Berti, K. Yagi, and N. Yunes, *Gen. Rel. Grav.* **50**, 46 (2018), arXiv:1801.03208 [gr-qc].
- [16] E. Berti, K. Yagi, H. Yang, and N. Yunes, *Gen. Rel. Grav.* **50**, 49 (2018), arXiv:1801.03587 [gr-qc].
- [17] Y.-F. Wang, R. Niu, T. Zhu, and W. Zhao, (2020), arXiv:2002.05668 [gr-qc].
- [18] M. Preto, I. Berentzen, P. Berczik, and R. Spurzem, *Astrophys. J.* **732**, L26 (2011).
- [19] E. Barausse, V. Cardoso, and P. Pani, *Proceedings, 10th International LISA Symposium: Gainesville, Florida, USA, May 18-23, 2014*, *J. Phys. Conf. Ser.* **610**, 012044 (2015), arXiv:1404.7140 [astro-ph.CO].
- [20] L. Barsotti, *Nature Astronomy* **2**, 619 (2018).
- [21] S. T. McWilliams, R. Caldwell, K. Holley-Bockelmann, S. L. Larson, and M. Vallisneri, (2019), arXiv:1903.04592 [astro-ph.HE].
- [22] B. P. Abbott *et al.* (LIGO Scientific, Virgo), *Astrophys. J.* **818**, L22 (2016), arXiv:1602.03846 [astro-ph.HE].
- [23] M. C. Miller and V. M. Lauburg, *Astrophys. J.* **692**, 917 (2009), arXiv:0804.2783 [astro-ph].
- [24] F. Antonini and H. B. Perets, *Astrophys. J.* **757**, 27 (2012), arXiv:1203.2938 [astro-ph.GA].
- [25] J. Hong and H. M. Lee, *Mon. Not. R. Astron. Soc.* **448**, 754 (2015), arXiv:1501.02717.
- [26] J. H. VanLandingham, M. C. Miller, D. P. Hamilton, and D. C. Richardson, *Astrophys. J.* **828**, 77 (2016), arXiv:1604.04948 [astro-ph.HE].
- [27] B.-M. Hoang, S. Naoz, B. Kocsis, F. A. Rasio, and F. Dosopoulou, *Astrophys. J.* **856**, 140 (2018), arXiv:1706.09896 [astro-ph.HE].
- [28] C. Petrovich and F. Antonini, *Astrophys. J.* **846**, 146 (2017), arXiv:1705.05848 [astro-ph.HE].
- [29] M. Arca-Sedda and A. Gualandris, *Mon. Not. Roy. Astron. Soc.* **477**, 4423 (2018), arXiv:1804.06116 [astro-ph.GA].
- [30] G. Fragione, E. Grishin, N. W. C. Leigh, H. Perets, and R. Perna, (2018), 10.1093/mnras/stz1651, arXiv:1811.10627 [astro-ph.GA].
- [31] I. Bartos, B. Kocsis, Z. Haiman, and S. Macutearka, *Astrophys. J.* **835**, 165 (2017), arXiv:1602.03831 [astro-ph.HE].
- [32] N. C. Stone, B. D. Metzger, and Z. Haiman, *Mon. Not. Roy. Astron. Soc.* **464**, 946 (2017), arXiv:1602.04226 [astro-ph.GA].
- [33] B. Mckernan *et al.*, *Astrophys. J.* **866**, 66 (2018), arXiv:1702.07818 [astro-ph.HE].

- [34] X. Chen, S. Li, and Z. Cao, *Mon. Not. Roy. Astron. Soc.* **485**, L141 (2019), arXiv:1703.10543 [astro-ph.HE].
- [35] K. Inayoshi, N. Tamanini, C. Caprini, and Z. Haiman, *Phys. Rev.* **D96**, 063014 (2017), arXiv:1702.06529 [astro-ph.HE].
- [36] A. Secunda, J. Bellovary, M.-M. Mac Low, K. E. S. Ford, B. McKernan, N. Leigh, and W. Lyra, *Astrophys. J.* **878**, 85 (2019), arXiv:1807.02859 [astro-ph.HE].
- [37] E. Addison, P. Laguna, and S. Larson, (2015), arXiv:1501.07856 [astro-ph.HE].
- [38] X. Chen and W.-B. Han, *Communications Physics* **1**, 53 (2018), arXiv:1801.05780 [astro-ph.HE].
- [39] Y. Kozai, *Astron. J.* **67**, 591 (1962).
- [40] M.L.Lidov, *Planet. Space Sci.* **9**, 719 (1962).
- [41] S. Naoz, *Annu. Rev. Astron. Astrophys.* **54**, 441 (2016), 1601.07175.
- [42] L. Wen, *Astrophys. J.* **598**, 419 (2003), arXiv:astro-ph/0211492 [astro-ph].
- [43] P. C. Peters and J. Mathews, *Phys. Rev.* **131**, 435 (1963).
- [44] S. Naoz, B. Kocsis, A. Loeb, and N. Yunes, *Astrophys. J.* **773**, 187 (2013), arXiv:1206.4316 [astro-ph.SR].
- [45] C. M. Will, *Phys. Rev.* **D89**, 044043 (2014), [Erratum: *Phys. Rev.* D91,no.2,029902(2015)], arXiv:1312.1289 [astro-ph.GA].
- [46] C. M. Will, *Phys. Rev. Lett.* **120**, 191101 (2018).
- [47] H. Lim and C. L. Rodriguez, (2020), arXiv:2001.03654 [astro-ph.HE].
- [48] Y. Fang and Q.-G. Huang, *Phys. Rev.* **D99**, 103005 (2019), arXiv:1901.05591 [gr-qc].
- [49] Y. Fang, X. Chen, and Q.-G. Huang, *Astrophys. J.* **887**, 210 (2019).
- [50] C. S. Reynolds, *Class. Quant. Grav.* **30**, 244004 (2013), arXiv:1307.3246 [astro-ph.HE].
- [51] C. S. Reynolds, *Space Sci. Rev.* **183**, 277 (2014), arXiv:1302.3260 [astro-ph.HE].
- [52] B. Liu, D. Lai, and Y.-H. Wang, *Astrophys. J.* **883**, L7 (2019), arXiv:1906.07726 [astro-ph.HE].
- [53] A. Einstein, L. Infeld, and B. Hoffmann, *Ann. Math.* **39**, 65 (1938).
- [54] A. R. de Sitter, W., *Mon. Not. R. Astron. Soc.* **77**, 155 (1916).
- [55] C. M. Will, *Phys. Rev.* **D96**, 023017 (2017), arXiv:1705.03962 [astro-ph.EP].
- [56] D. A. Nichols *et al.*, *Phys. Rev.* **D84**, 124014 (2011), arXiv:1108.5486 [gr-qc].
- [57] K. S. Thorne and J. B. Hartle, *Phys. Rev.* **D31**, 1815 (1984).
- [58] E. Poisson and C. M. Will, Cambridge University Press (2014).
- [59] S. Naoz, W. M. Farr, Y. Lithwick, F. A. Rasio, and J. Teyssandier, *Nature* **473**, 187 (2011), arXiv:1011.2501 [astro-ph.EP].
- [60] Y. Lithwick and S. Naoz, *Astrophys. J.* **742**, 94 (2011), arXiv:1106.3329 [astro-ph.EP].
- [61] P. B. Ivanov, A. G. Polnarev, and P. Saha, *Mon. Not. R. Astron. Soc.* **358**, 1361 (2005).
- [62] D. Merritt and E. Vasiliev, *Astrophys. J.* **726**, 61 (2011), arXiv:1005.0040 [astro-ph.GA].